Mechanically manipulate glymphatic transport by focused ultrasound combined with microbubbles

Dezhuang Ye[1#], Si Chen[1#], Yajie Liu[1], Charlotte Weixel[1], Zhongtao Hu[1], Jinyun Yuan[1], and Hong Chen[1,2,3,4*]

1. Department of Biomedical Engineering, Washington University in St. Louis, Saint Louis, MO 63130, USA.

2. Department of Radiation Oncology, Washington University School of Medicine, Saint Louis, MO 63130, USA.

3. Department of Neurosurgery, Washington University School of Medicine, St. Louis, MO, 63110, USA

4. Division of Neurotechnology, Washington University School of Medicine, Saint Louis, MO, 63110, USA

# These authors contributed equally.

* Address correspondence to: Hong Chen, Ph.D., Department of Biomedical Engineering and Radiation Oncology, Washington University in St. Louis, 4511 Forest Park Ave., St. Louis, MO, 63108, USA. Telephone: 314-454-7742. Email: hongchen@wustl.edu

This PDF file includes:

Figures S1 to S6
Legends for Movies S1 to S11

Other supplementary materials for this manuscript include the following:

Movies S1 to S11

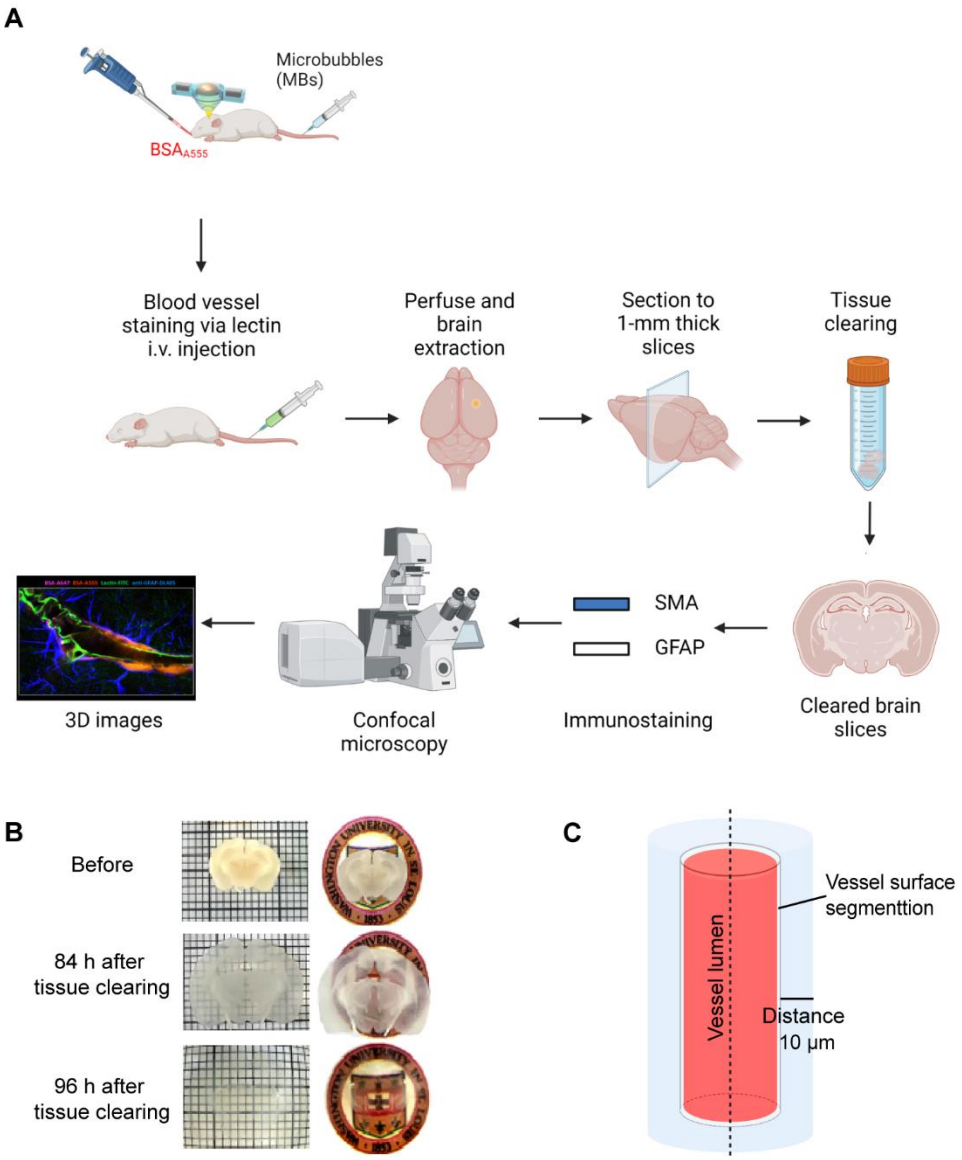

Fig. S1. (A) Illustration of experimental workflow. (B) Pictures of a 1-mm thick coronal brain section undergoing optically clearing using an established method (H. Hama, et al., Nat. Neurosci. 2015). (C) Illustration of single vessel segmentation for quantifying albumin fluorescence intensity in the perivascular space.

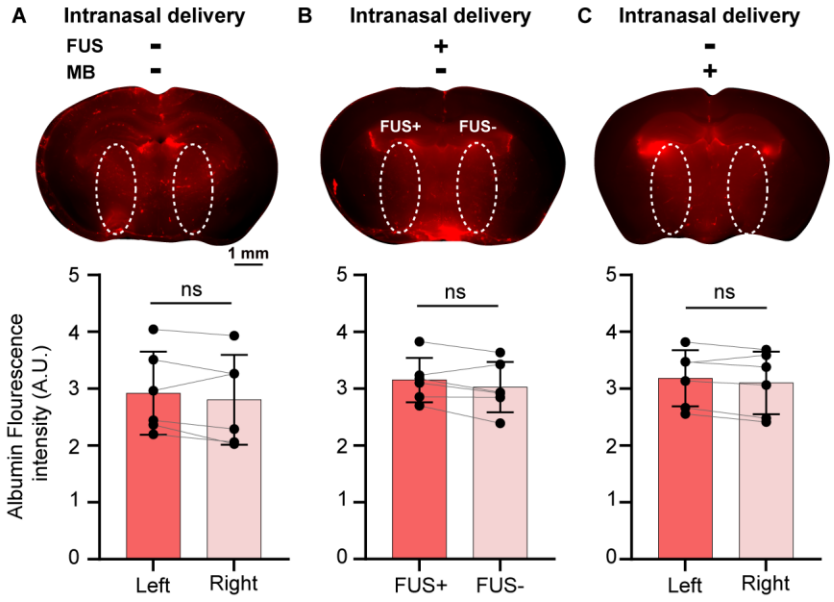

Fig. S2. Control studies verified that both FUS and MB were needed to enhance agent transport. Representative fluorescent image of albumin tracer in a 1-mm thick brain section at low magnification (2×) from control groups (top) and corresponding fluorescence quantification (bottom) prior to tissue clearance. (A) Intranasal delivery of the albumin tracer without FUS or microbubbles, (B) intranasal delivery of the albumin tracer with FUS but without microbubbles, and (C) intranasal delivery of the albumin tracer with microbubbles but without FUS. The fluorescence intensity was measured within the region of interest (ROI) defined by the white dashed line.

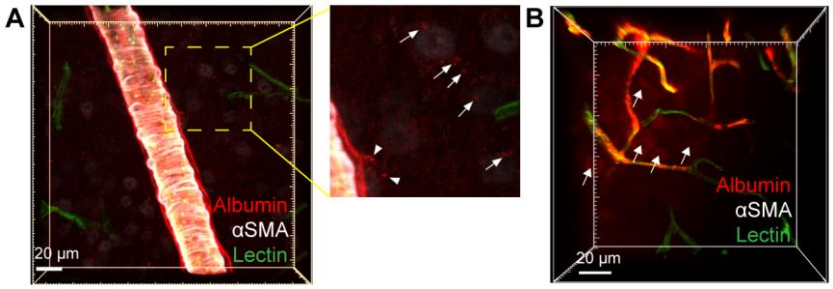

Fig. S3. FUSMB enhanced albumin transportation into the interstitial space. Albumin extravasation from the perivascular space into the interstitial space was observed in arterioles (A) and capillaries (B) in the FUS-treated brain region. For (A), a zoomed-in image within the yellow box is shown on the right, and white arrows mark the albumin tracer in the interstitial space. For (B), the white arrows mark the albumin tracer in the interstitial space. Scale bars = 20 μm.

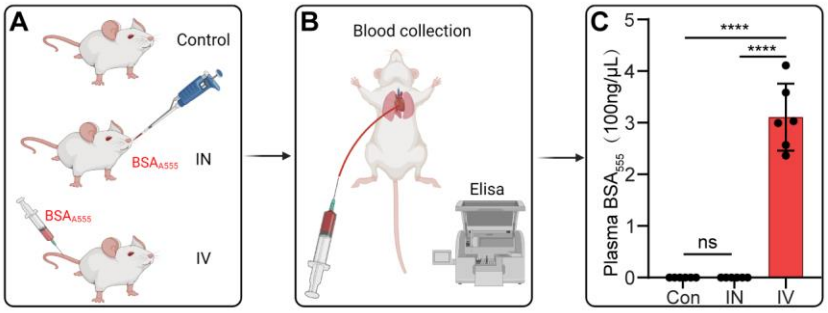

Fig. S4. Quantification of Alexa Fluor 555-albumin concentration in the blood. (A) Alexa Fluor 555-albumin was administered to two groups of mice via intranasal administration (IN) and intravenous injection (IV) at the same dose. A control group without albumin injection was included. (B) Mouse blood was collected via cardiac puncture into BD Vacutainer K2 EDTA tubes (Becton Dickinson, Franklin Lakes, NJ, USA) at 45 min post IN or IV delivery and centrifuged at 3000×g for 10 minutes at 4°C to separate plasma. Alexa Fluor 555-albumin (13 mg/ml) was serially diluted 10-fold for standards. Standards and 2-fold diluted plasma samples were loaded onto FLUOTRAC™ microplates (Greiner Bio-One, Monroe, NC, USA). Fluorescence signals were measured using a SpectraMax® i3x (Molecular Devices, San Jose, CA, USA). The concentration of Alexa Fluor 555-albumin in plasma was calculated based on the standard curve for Alexa Fluor 555-albumin. The fluorescence intensity of Alexa Fluor 555 was used to quantify the concentration of Alexa Fluor 555-albumin in the blood. (C) Statistical analysis was performed by one-way ANOVA followed by Tukey's multiple comparisons test using GraphPad Prism (version 9.4.1, La Jolla, CA, USA). No significant difference was found in the blood levels of Alexa Fluor 555-albumin between the control and IN groups, while the Alexa Fluor 555-albumin concentration in the blood after IN is more than 5,000x lower compared to that after IV (****P<0.0001).

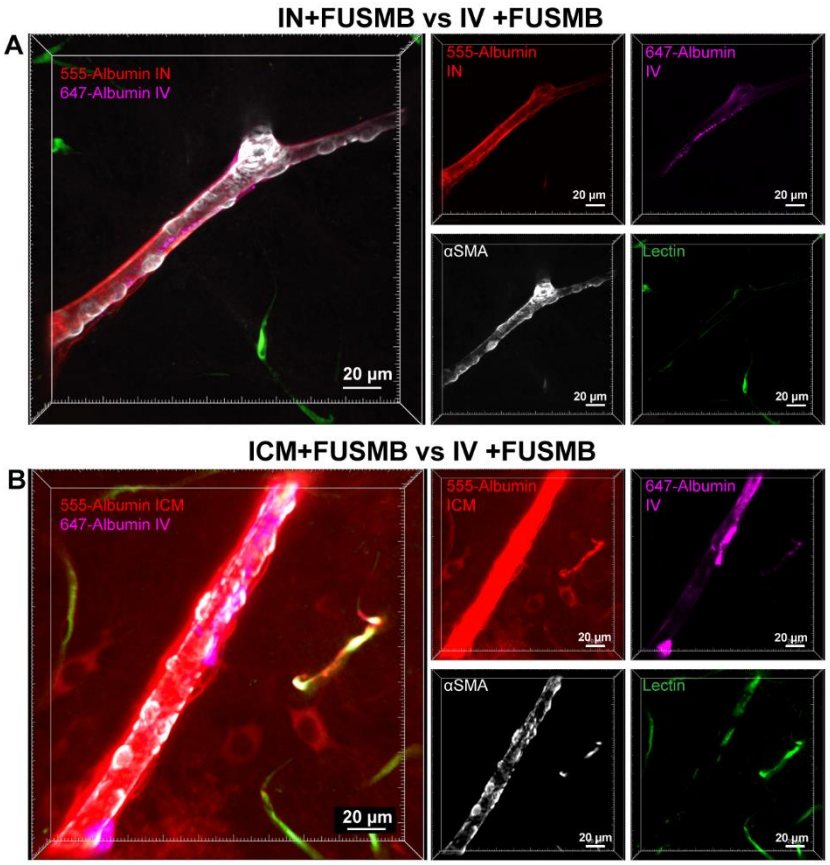

Fig. S5. 3D confocal microscopy images obtained using a 20× objective showed that the IN-administered agents with FUSMB displayed continuous distribution along the blood vessels, similar to that of ICM+FUSMB but different from that of intravenous injection (IV)+FUSMB. (A) Comparison of the distribution pattern of IN-administrated Alexa Fluor 555-albumin (red) and IV-injected Alexa Fluor 647-albumin (magenta) followed by FUSMB treatment in the same mice, IN-administrated albumin exhibited continuous distributions along the vessel. In contrast, IV-injected albumin showed discontinuous distribution along the vessel wall. (B) Comparison of the distribution pattern of ICM-injected Alexa Fluor 555-albumin (red) and IV-injected of Alexa Fluor 647-albumin (magenta) followed by FUSMB treatment in the same mouse, ICM-injected albumin exhibited continuous distributions along the vessel. In contrast, IV-injected albumin showed discontinuous distribution along the vessel wall (image size: 200 × 200 × 28 μm^3).

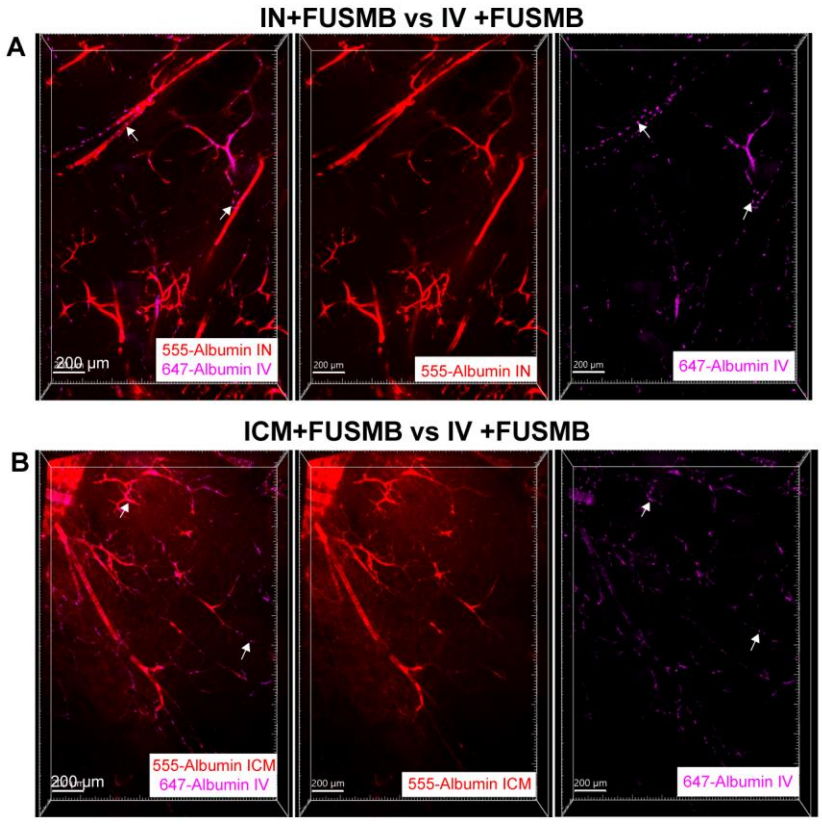

Fig. S6. 3D confocal microscopy images captured using a 5× objective, covering a volume of 1.52 × 2.24 × 0.26 mm³ at the FUS-treated brain region, display different distribution patterns of albumin following IN compared to IV and ICM after FUSMB treatment. (A) Comparison of distribution patterns for IN-administered Alexa Fluor 555-albumin (red) and IV-injected Alexa Fluor 647-albumin (magenta) following FUSMB treatment in the same mouse. (B) Comparison of distribution patterns for ICM-injected Alexa Fluor 555-albumin (red) and IV-injected Alexa Fluor 647-albumin (magenta) following FUSMB treatment in the same mice. White arrows point to the dispersed IV-injected Alexa Fluor 647-albumin.

Movie S1: Three-dimensional view of the image shown in Fig. 2A. Red, albumin; green, lectin; blue, GFAP.

Movie S2: Three-dimensional view of the image shown in Fig. 2C. Red, albumin; green, lectin; blue, GFAP.

Movie S3: Three-dimensional view of the image shown in Fig. 2E. Red, albumin; green, lectin; blue, GFAP.

Movie S4: Three-dimensional view of the image shown in Fig. 3A. Red, albumin; green, lectin; white, αSMA.

Movie S5: Three-dimensional view of the image shown in Fig. 4A. Red, albumin; green, lectin; white, αSMA.

Movie S6: Three-dimensional view of the image shown in Fig. 5A. Red, albumin; green, lectin; white, αSMA

Movie S7: Three-dimensional view of the image shown in Fig. 5C. Red, albumin; green, lectin; white, αSMA

Movie S8: Three-dimensional view of the image shown in Fig. S3A. Red, albumin; green, lectin; white, αSMA

Movie S9: Three-dimensional view of the image shown in Fig. S3B. Red, albumin; green, lectin; white, αSMA

Movie S10: Three-dimensional view of the image shown in Fig. S5A. Red, albumin; green, lectin; white, αSMA

Movie S11: Three-dimensional view of the image shown in Fig. S5B. Red, albumin; green, lectin; white, αSMA